Kinetic Trapping of Rylene Diimide Covalent Organic Cages

Sergey Fisher[a‡], Hsin-Hua Huang[b‡], Luise Sokoliuk[b], Alessandro Prescimone[b], Olaf Fuhr[c], Tomáš Šolomek*[a,b]

[a] Van 't Hoff Institute for Molecular Sciences, University of Amsterdam, Science Park 904, NL-1098 XH Amsterdam, The Netherlands.

[b] Department of Chemistry, University of Basel, St. Johanns-Ring 19, CH-4056 Basel, Switzerland.

[c] Institute of Nanotechnology and Karlsruhe Nano Micro Facility, Karlsruhe Institute of Technology, Kaiserstraße 12, DE-76131 Karlsruhe, Germany.

Supporting Information Placeholder

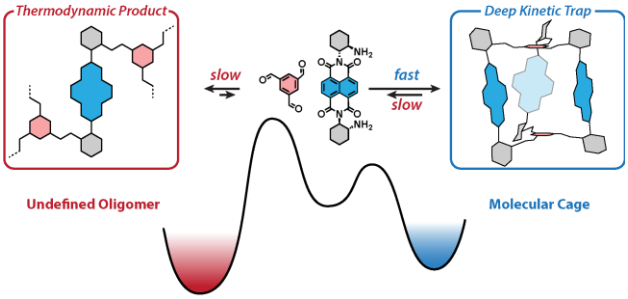

Rylene diimide cages formed under kinetic control

ABSTRACT: Formation of imine organic cages relies on error-correction of dynamic covalent chemistry. Here, we demonstrate kinetically-trapped rylene diimide cages formed in high yields and we investigate the effect of substituents on their formation kinetics and stability. Thereby, we identified that alkoxy groups in triformylbenzene, used to stabilize covalent organic cages or COFs, act as stereoelectronic chameleons. We underscore critical factors governing the chemistry of kinetically-trapped imine assemblies like sterics, electronics, catalysis, and water concentration.

Multicomponent molecular assembly guided by dynamic covalent chemistry (DCC) is a powerful tool to create intricate two and three-dimensional structures, such as macrocycles[1–3], cages[4,5], molecular knots[6], or covalent organic frameworks[7] in a single step. The extensive array of accomplished porous organic cages (POC) promises that their structures can be tailored via DCC to achieve specific requirements.[8–12] Despite this versatility, accurately predicting the synthetic outcome in POC synthesis remains a considerable challenge in the field. The reversible nature of DCC implies that the products are formed under thermodynamic control[13], which in principle allows for predictions by comparing the heats of formation of POCs.[14–18] Jelfs and Cooper *et al.* demonstrated such computational workflows using density functional theory (DFT) that agreed well with the experiments and helped rationalizing the composition of complex product mixtures. Despite the success of this approach, there are cases that underscore the significance of kinetics in the formation of POCs. Here, alternative reaction pathways may lead to unwanted by-products, *e.g.*, oligomers, or the POCs themselves might represent kinetically trapped products. Furthermore, hard-to-predict circumstances, such as kinetic trapping through precipitation, can pose significant challenges in the synthesis design. Computing kinetic pathways in POC formation is even more intricate than accurate calculation of heat of formation. Yet, the kinetic factors could be leveraged to allow access to novel structures, such as asymmetric cages, and diverse dynamic covalent libraries that can be temporarily conserved out of equilibirum. Therefore, identification of POCs that are formed as kinetic traps in high yields is of considerable importance.[19] They allow to study the factors that govern their formation and kinetic or thermodynamic stability informing future design. However, the lack of reversiblity in the kinetic control fails to provide the error correction mechanism, which is typically detrimental to the reaction yield.

Recently, we reported the high-yielding synthesis, textural and optoelectronic properties of a family of electron-poor rylene diimide POCs.[17,20,21] Light excitation of naphthalene-1,4:5,8-bis(dicarbox-imide) (NDI) cage (**1a**, Figure 1) created a long-lived charge separated state with an electron residing on one NDI unit and a hole on the bridge.[17,22] Such long-lived states could be utilized in photocatalysis, which motivated us to synthesize analogous cages **1b** and **1c** with strong electron donors in the bridges to manipulate the excited state dynamics.

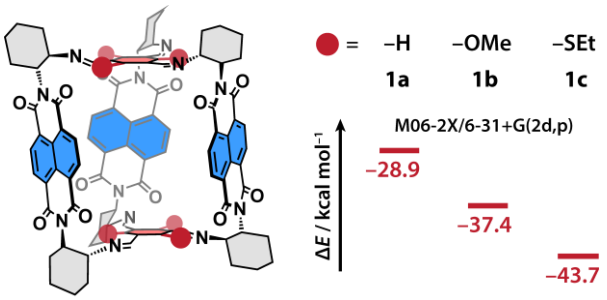

Figure 1. NDI cages with 1,3,5-iminoarene bridges with H (**1a**), Me–O (**1b**), and Et–S (**1c**) substituents. The heats of cage formation (red) are shown in kcal mol^{-1} (M06-2X/6-31+G(2d,p) level of theory).

Table 1. Optimization of reaction conditions for the synthesis of cages **1a–c** and **2a–c**.

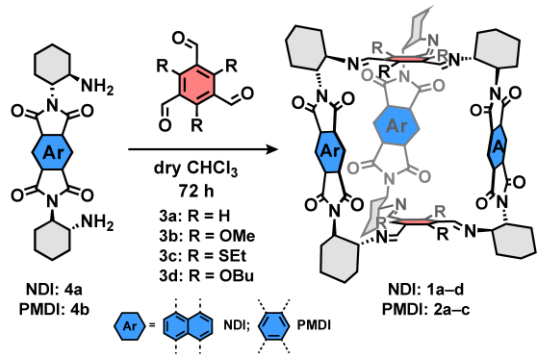

Entry	Additive	T / °C	Yield / %[a]
1	–	80	<20 (20[b])
2	10mol% $Sc(OTf)_3$	25	8
3	6 equiv. *p*-TsOH, excess NEt_3	25	<8
4	–	25	48 (85[b], 45[c])

[a] The yield of **1b** is based on isolated and dried product after purification by HPLC. [b] The yield in brackets corresponds to **2b**. [c] The yield in brackets corresponds to **1d**. See the SI for a complete list of conditions.

The synthesis of **1a** achieved by condensation of 1,3,5-triformylbenzene (**3a**, Table 1) and the corresponding enantiomerically pure NDI diamine **4a** in high yield (60%; dry $CHCl_3$: c_{H2O} = 7 ppm, 80 °C, 72 h)[20] could be successfully predicted by the computational workflow from recent literature[16,23,24] (Figure 1). The same calculations also suggested that both **1b** and **1c** would be formed in high yields because their formation was markedly more exothermic than that of **1a**. We synthesized the required tritopic aldehydes **3** and reacted them with **4a** in dry $CHCl_3$ at elevated temperature to establish the equilibrium. Only a small amount of impure **1b** (Table 1, entry 1) and no **1c** could be detected even after prolonged reaction time (14 days). To improve their synthesis, we added $Sc(OTf)_3$ as a catalyst, or we started the synthesis from ditosylate salt of **4a** in anhydrous chloroform at 25 °C (Table 1, entries 2–3). Similar to the initial attempts, no **1c** could be detected and the yield of **1b** decreased. This suggests

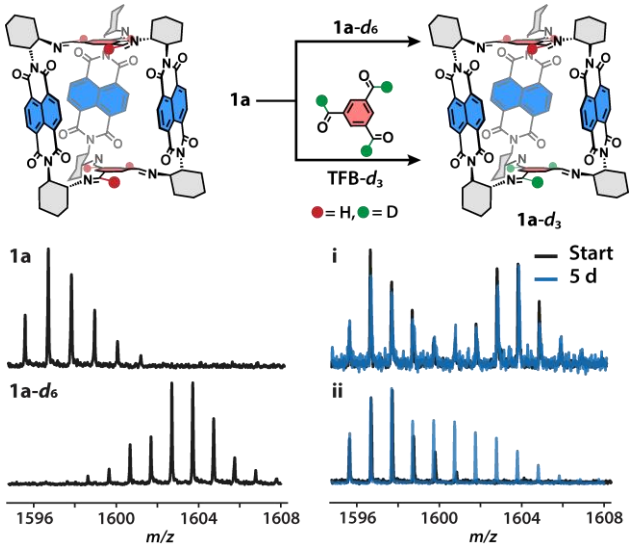

Figure 2. Scrambling of **1a** with isotopologue **1a-*d*$_6$** (top) or deuterated **3a** (bottom) to obtain the mixed **1-*d*$_3$**. MALDI-MS show the isotopic pattern for **1a** and **1-*d*$_6$** as well as (*i*) the scrambling of **1a** and **1-*d*$_6$** and (*ii*) the reaction of **1a** with **3a-*d*$_3$** in water-saturated $CHCl_3$.

that formation of the target cages might face a kinetic barrier to establish the equilibrium. Consequently, we attempted to overcome the reaction barrier by a combination of $Sc(OTf)_3$ and elevated temperature (80 °C), but the reaction resulted in an unidentifiable product mixture with no sign of cage **1c**. To our surprise, the synthesis of **1b** from **4a** and **3b** at 25 °C in the absence of any Brønstedt or Lewis acid catalyst improved the purity of the crude product mixture markedly and provided **1b** in 48% yield after purification (Table 1, entry 4). The outcome of this experiment was unexpected since cage **1a** can be formed at elevated temperatures in excellent yields.[17] We repeated the same set of experiments with PMDI diamine **4b** because we observed previously that **2a** formed in a cleaner process than **1a**. However, attempts to form **2b** paralleled the observations with **1b**, and formation of **2b** exhibited excellent 85% yield after purification by HPLC only at 25 °C without additives.[20] Notably, a significant portion of the observed products were insoluble, likely oligomeric, by-products that we could not characterize. All our observations therefore imply that rylene diimide cages **1** and **2** probably represent kinetic rather than thermodynamic products in chloroform. Although the formation of **1c** appears to proceed via a high barrier, all other cages could be isolated in high yields when synthesized at room temperature without the error-correction mechanism of DCC.

To test the dynamic nature of the rylene cages, we synthesized the deuterated isotopologue **1a-*d*$_6$** with deuterium atoms in the imine positions in the bridge (Figure 2) and examined its scrambling with **1a**. Both cages were mixed in $CHCl_3$ for 96 h and the reaction mixture was analysed with matrix-assisted laser desorption ionization time of flight mass spectrometry. Regardless of the water content (7 and >700 ppm), temperature (25 and 60 °C), and the presence of acid catalyst

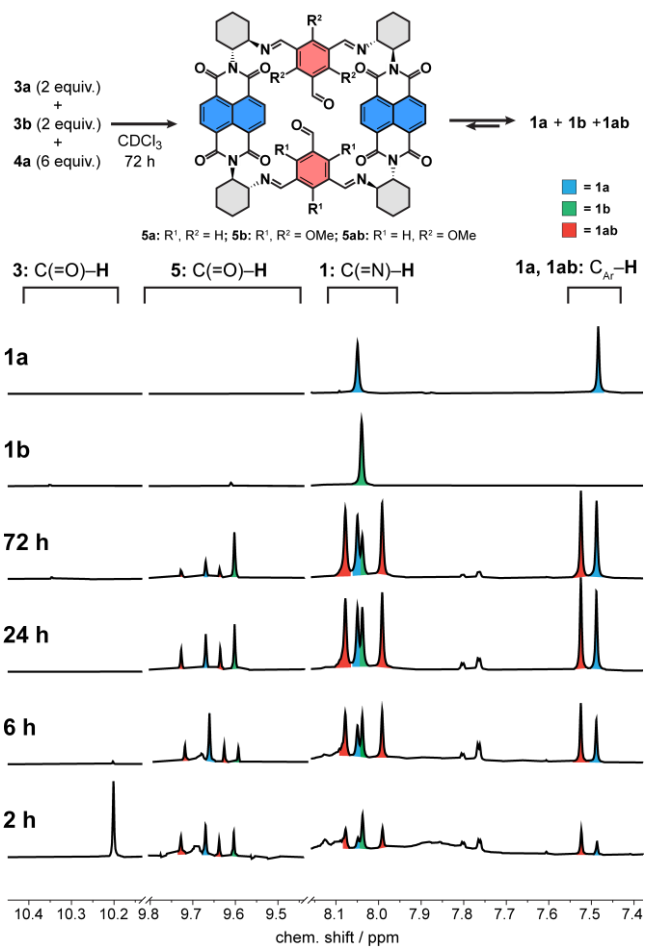

Figure 3. Kinetic self-sorting of **3a** and **3b** with **4a** in $CDCl_3$.

(TFA, 1 mol%), we did not observe formation of **1a-*d*$_3$** (Figure 2 and Fig. S42), population of which should reach ~50% in an equilibrium. We only noticed an increase in the signal-to-noise ratio over the course of the experiment hinting at a slow decomposition of the cages under the selected conditions. The absence of the imine metathesis proves unambiguously that cage **1a** is formed as a kinetic trap.

The substituents in the bridging units in **1** provide an opportunity to investigate the formation and stability of these kinetically trapped POCs. Previously, Banerjee and co-workers reported that the steric bulk and electronic properties of the MeO groups in **3b** endowed the classical Cooper's [6+4]-cage CC3 with exceptional kinetic stability.[5,25] However, cages **1b** and **2b** seem to be more sensitive to the environment than **1a** and **2a**. The electron-donating nature and the size of MeO and EtS groups (Hammett $\sigma_p < 0$) suggest that they increase the barrier for cage formation, and also make them thermodynamically more stable.[26] The former assumes an amine nucleophilic attack as the rate-limiting step, as showed previously when imine formation and metathesis occur in a dry organic solvent without a catalyst.[27,28] The latter is reflected in the computed heats of formation (Figure 1). The electronic and steric factors clearly prevent formation of **1c**. However, replacing MeO for bulkier BuO groups in the trialdehyde **3d** (Table 1) did not prevent formation of the corresponding cage

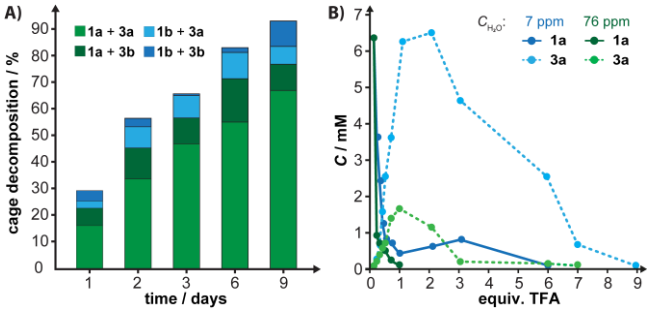

Figure 4. (A) Cages decomposition in $CDCl_3$ upon addition of **3** or (B) 2,2,2-trifluoroacetic acid.

1d at room temperature (45% yield) despite a markedly stronger electron donor than the EtS group. X-ray diffraction analysis of single crystals of **1b** and **1d** revealed that all three alkoxy substituents are significantly rotated (>74°, Figures S39-S41) out of the arene bridge plane. This is confirmed by DFT calculations that show similar effect in the trialdehyde **3b** (83.4°, Figure S41). Note that the rotation not only dimishes the electron-donating ability of MeO groups, it, in fact, turns them into electron acceptors. Such stereoelectronic effect has been observed and applied to control reactivity before.[29,30] We tested this notion in a kinetic competition experiment by mixing 2 equiv. of **3a** and **3b** each and 6 equiv. of **4a** in $CDCl_3$ and monitoring the reaction progress by ^{1}H NMR (Figure 3). While **3b** was consumed entirely within 2 h of the reaction, traces of **3a** were still present after 6 h. Small amounts of **1a** and **1b** were already detected after 2 h together with a product that we assigned to a cage having both type of bridges (**1ab**). Early on, the amount of formed cages follows the number of **3b** incorporated in the cage: **1b** > **1ab** > **1a**. In addition, a set of four resonances (9.60–9.75 ppm) suggests the presence of macrocyclic [2+2] condensates **5** (Figure 3) that we tentatively assigned following previously identified **5a** observed upon partial hydrolysis of **1a**.[17] Their concentration remained low during the 120 h experimental window except for **5b** (Figure S43). The concentration of all cages steadily increased in time, but only that of **1b** reached a maximum (~24 h), after which it slowly decomposed with concomitant increase of **5b**. Cages **1a** and **1ab** remained stable until the end of the experiment. The reaction mixture turned slightly turbid after 48 h, likely due to formation of insoluble oligomers. Independent samples of **1a** and **1b** in dry or wet $CDCl_3$ (Figure S53) did not show any sign of cage decomposition in 30 days.[17] A few key conclusions can thus be drawn: (*i*) **3b** is indeed more electrophilic than **3a**, (*ii*) a single MeO bridge does not compromise the cage stability and (*iii*) decomposition of **1b** to **5b** must be catalyzed. It follows from (*ii*) that cage hydrolysis does not proceed via removing the bridge, but by opening a cage rung releasing **4a**, *i.e.*, the [2+2] macrocycles **5** are intermediates in cages formation.[17]

We probed if aldehydes present in the solution could cap a free amine after one of the cage imines gets hydrolyzed preventing it from reforming the cage. Thereby, aldehydes would catalyse cage decomposition formally releasing **4a**–aldehyde condensates that might be dynamic due to absence of a rung. We compared the reaction progress of solutions of **1a** and **1b** upon addition of 6 equiv. of **3a** or **3b** in $CDCl_3$ (Figure 4A, c_{H2O} ~ 70 ppm, 25°C). We observed that in all cases the cages

decomposed in the course of days, but all at different relative rates: **1b**,**3b** ≈ **1b**,**3a** > **1a**,**3b** > **1a**,**3a**. The observed trend reinforces that **3b** is more electrophilic than **3a** and confirms that **1a** is kinetically more stable than **1b** because it incorporates two bridges from less electrophilic trialdehyde. The decomposition also proceeds with catalytic amount of **3**, although at a slower rate (Figure S47). We do not observe formation of **1ab** when **1a** (or **1b**) was reacted with **3b** (**3a**) irrespective of water content in $CDCl_3$ (Figures S48-S51). We only observe the expected formation of **5a** that is continuously converted to **5b** and **5ab** (Figures S46-S52). The excess of aldehydes scavenges all released **4a**, preventing cage reformation. Yet, MS analysis revealed the presence of **1a**-d_3 upon mixing of **1a** and excess **3a**-d_3 (Figure 2).

Cage **1a** decomposes by a stepwise addition of TFA (probed after ~10 min; Figure 4B) that promotes DCC. TFA initiated formation of **5a** and additional **4a**-aldehyde condensates that we did not identify. Their concentration was relatively independent of the added TFA (<2 equiv.), however, that of **1a** gradually decreased (Figure S54-S55). Simultaneously, concentration of **3a** increased, reaching a maximum at ~1–2 equiv. of TFA before gradually declining. Consumption of **3a** correlated with the formation of precipitates, suggesting its incorporation into insoluble oligomers. The reaction progress depended critically on water. Under dry conditions (7 ppm H_2O), catalytic amount of TFA did not fully decompose **1a** (even at 24 h, Figure S56) and produced **3a** at a higher concentration than in the water-enriched (76 ppm) sample. A few equivalents of TFA were necessary to fully consume **1a** in dry $CDCl_3$, while the process appeared catalytic at higher water content. In **1b**, 0.1 equiv. of TFA resulted in its complete decomposition, even under anhydrous conditions (Figure S57). These experiments underscore the unusual kinetic stability of **1a** and show that alkoxy groups in **3** may protect a cage only in a heterogenous sample. We also argue that water concentration, an often underestimated parameter in POC synthesis, may critically affect reaction kinetics, and possibly establish the kinetic or thermodynamic control of the process.

In conclusion, we demonstrated that [3+2] rylene diimide cages are kinetically trapped, yet formed in high yields despite the absence of error-correction mechanism of imine DCC. We showed how their rate of formation and kinetic stability are affected by bridge substitution, which helped us identify [2+2] macrocyclic intermediates in their formation/decomposition. These macrocycles might equally be kinetically trapped, representing exciting targets to investigate as key intermediates to accomplish asymmetric covalent organic cages in high yields. This study thus uncovers factors that govern formation and stability of kinetically-trapped molecular imine assemblies, which will inform the design of future three-dimensional systems locked out-of-equilibrium.

ASSOCIATED CONTENT

Supporting Information

The Supporting Information is available free of charge on the ACS Publications website.

Experimental procedures, characterization data, computational details, and crystal data (PDF)

Accession Codes

CCDC 2145025 and CCDC 2373256 contain the supplementary crystallographic data for this paper. These data can be obtained free of charge via www.ccdc.cam.ac.uk/data_request/cif, or by emailing data_request@ccdc.cam.ac.uk, or by contacting The Cambridge Crystallographic Data Centre, 12 Union Road, Cambridge CB2 1EZ, UK; fax: +44 1223 336033.

AUTHOR INFORMATION

Corresponding Author

Tomáš Šolomek – Van 't Hoff Institute for Molecular Sciences, University of Amsterdam, Science Park 904, NL-1098 XH Amsterdam, The Netherlands. E-mail: t.solomek@uva.nl

Authors

Sergey Fisher – Van 't Hoff Institute for Molecular Sciences, University of Amsterdam, Science Park 904, NL-1098 XH Amsterdam, The Netherlands.

Hsin-Hua Huang – Department of Chemistry, University of Basel, St. Johanns-Ring 19, CH-4056 Basel, Switzerland.

Luise Sokoliuk – Department of Chemistry, University of Basel, St. Johanns-Ring 19, CH-4056 Basel, Switzerland.

Alessandro Prescimone – Department of Chemistry, University of Basel, St. Johanns-Ring 19, CH-4056 Basel, Switzerland.

Author Contributions

The manuscript was written through contributions of all authors. All authors have given approval to the final version of the manuscript. ‡These authors contributed equally.

Notes

The authors declare no competing financial interest.

ACKNOWLEDGMENT

The authors are grateful for the financial support from the European Research Council (ERC, Grant Agreement No. 949397), the Swiss National Science Foundation (SNSF, PZ00P2_174175), the University of Amsterdam, and the University of Basel.

REFERENCES

(1) Kryschenko, Y. K.; Seidel, S. R.; Arif, A. M.; Stang, P. J. Coordination-Driven Self-Assembly of Predesigned Supramolecular Triangles. *J. Am. Chem. Soc.* **2003**, *125* (17), 5193–5198. https://doi.org/10.1021/ja030018k.

(2) Hartley, C. S.; Elliott, E. L.; Moore, J. S. Covalent Assembly of Molecular Ladders. *J. Am. Chem. Soc.* **2007**, *129* (15), 4512–4513. https://doi.org/10.1021/ja0690013.

(3) Fujita, M.; Oguro, D.; Miyazawa, M.; Oka, H.; Yamaguchi, K.; Ogura, K. Self-Assembly of Ten Molecules into Nanometre-Sized Organic Host Frameworks. *Nature* **1995**, *378* (6556), 469–471. https://doi.org/10.1038/378469a0.

(4) Lee, S.; Yang, A.; Moneypenny, T. P. I.; Moore, J. S. Kinetically Trapped Tetrahedral Cages via Alkyne Metathesis. *J. Am. Chem. Soc.* **2016**, *138* (7), 2182–2185. https://doi.org/10.1021/jacs.6b00468.

(5) Tozawa, T.; Jones, J. T. A.; Swamy, S. I.; Jiang, S.; Adams, D. J.; Shakespeare, S.; Clowes, R.; Bradshaw, D.; Hasell, T.; Chong, S. Y.; Tang, C.; Thompson, S.; Parker, J.; Trewin, A.; Bacsa, J.; Slawin, A. M. Z.; Steiner, A.; Cooper, A. I. Porous Organic Cages. *Nature Mater* **2009**, *8* (12), 973–978. https://doi.org/10.1038/nmat2545.

(6) Ponnuswamy, N.; Cougnon, F. B. L.; Clough, J. M.; Pantoş, G. D.; Sanders, J. K. M. Discovery of an Organic Trefoil Knot. *Science* **2012**, *338* (6108), 783–785. https://doi.org/10.1126/science.1227032.

(7) Côté, A. P.; Benin, A. I.; Ockwig, N. W.; O'Keeffe, M.; Matzger, A. J.; Yaghi, O. M. Porous, Crystalline, Covalent Organic Frameworks. *Science* **2005**, *310* (5751), 1166–1170. https://doi.org/10.1126/science.1120411.

(8) Hong, S.; Rohman, Md. R.; Jia, J.; Kim, Y.; Moon, D.; Kim, Y.; Ko, Y. H.; Lee, E.; Kim, K. Porphyrin Boxes: Rationally Designed Porous Organic Cages. *Angew. Chem. Int. Ed.* **2015**, *54* (45), 13241–13244. https://doi.org/10.1002/anie.201505531.

(9) Ding, H.; Yang, Y.; Li, B.; Pan, F.; Zhu, G.; Zeller, M.; Yuan, D.; Wang, C. Targeted Synthesis of a Large Triazine-Based [4+6] Organic Molecular Cage: Structure, Porosity and Gas Separation. *Chem. Commun.* **2015**, *51* (10), 1976–1979. https://doi.org/10.1039/C4CC08883B.

(10) Mitra, T.; Jelfs, K. E.; Schmidtmann, M.; Ahmed, A.; Chong, S. Y.; Adams, D. J.; Cooper, A. I. Molecular Shape Sorting Using Molecular Organic Cages. *Nat. Chem.* **2013**, *5* (4), 276–281. https://doi.org/10.1038/nchem.1550.

(11) Hussain, M. W.; Giri, A.; Patra, A. Organic Nanocages: A Promising Testbed for Catalytic CO2 Conversion. *Sustainable Energy Fuels* **2019**, *3* (10), 2567–2571. https://doi.org/10.1039/C9SE00394K.

(12) Liu, M.; Chen, L.; Lewis, S.; Chong, S. Y.; Little, M. A.; Hasell, T.; Aldous, I. M.; Brown, C. M.; Smith, M. W.; Morrison, C. A.; Hardwick, L. J.; Cooper, A. I. Three-Dimensional Protonic Conductivity in Porous Organic Cage Solids. *Nat. Commun.* **2016**, *7* (1), 12750. https://doi.org/10.1038/ncomms12750.

(13) Rowan, S. J.; Cantrill, S. J.; Cousins, G. R. L.; Sanders, J. K. M.; Stoddart, J. F. Dynamic Covalent Chemistry. *Angew. Chem. Int. Ed.* **2002**, *41* (6), 898–952. https://doi.org/10.1002/1521-3773(20020315)41:6<898::AID-ANIE898>3.0.CO;2-E.

(14) Greenaway, R. L.; Santolini, V.; Bennison, M. J.; Alston, B. M.; Pugh, C. J.; Little, M. A.; Miklitz, M.; Eden-Rump, E. G. B.; Clowes, R.; Shakil, A.; Cuthbertson, H. J.; Armstrong, H.; Briggs, M. E.; Jelfs, K. E.; Cooper, A. I. High-Throughput Discovery of Organic Cages and Catenanes Using Computational Screening Fused with Robotic Synthesis. *Nat Commun* **2018**, *9* (1), 2849. https://doi.org/10.1038/s41467-018-05271-9.

(15) Berardo, E.; Greenaway, R. L.; Turcani, L.; Alston, B. M.; Bennison, M. J.; Miklitz, M.; Clowes, R.; Briggs, M. E.; Cooper, A. I.; Jelfs, K. E. Computationally-Inspired Discovery of an Unsymmetrical Porous Organic Cage. *Nanoscale* **2018**, *10* (47), 22381–22388. https://doi.org/10.1039/C8NR06868B.

(16) Santolini, V.; Miklitz, M.; Berardo, E.; Jelfs, K. E. Topological Landscapes of Porous Organic Cages. *Nanoscale* **2017**, *9* (16), 5280–5298. https://doi.org/10.1039/C7NR00703E.

(17) Šolomek, T.; Powers-Riggs, N. E.; Wu, Y.-L.; Young, R. M.; Krzyaniak, M. D.; Horwitz, N. E.; Wasielewski, M. R. Electron Hopping and Charge Separation within a Naphthalene-1,4:5,8-Bis(Dicarboximide) Chiral Covalent Organic Cage. *J. Am. Chem. Soc.* **2017**, *139* (9), 3348–3351. https://doi.org/10.1021/jacs.7b00233.

(18) Greenaway, R. L.; Santolini, V.; Pulido, A.; Little, M. A.; Alston, B. M.; Briggs, M. E.; Day, G. M.; Cooper, A. I.; Jelfs, K. E. From Concept to Crystals via Prediction: Multi-Component Organic Cage Pots by Social Self-Sorting. *Angew. Chem. Int. Ed.* **2019**, *58* (45), 16275–16281. https://doi.org/10.1002/anie.201909237.

(19) Greenlee, A. J.; Wendell, C. I.; Cencer, M. M.; Laffoon, S. D.; Moore, J. S. Kinetic and Thermodynamic Control in Dynamic Covalent Synthesis. *Trends Chem.* **2020**, *2* (12), 1043–1051. https://doi.org/10.1016/j.trechm.2020.09.005.

(20) Huang, H.-H.; Song, K. S.; Prescimone, A.; Aster, A.; Cohen, G.; Mannancherry, R.; Vauthey, E.; Coskun, A.; Šolomek, T. Porous Shape-Persistent Rylene Imine Cages with Tunable Optoelectronic Properties and Delayed Fluorescence. *Chem. Sci.* **2021**, *12* (14), 5275–5285. https://doi.org/10.1039/D1SC00347J.

(21) Huang, H.-H.; Šolomek, T. Photochemistry Meets Porous Organic Cages. *Chimia* **2021**, *75* (4), 285–285. https://doi.org/10.2533/chimia.2021.285.

(22) Aster, A.; Rumble, C.; Bornhof, A.-B.; Huang, H.-H.; Sakai, N.; Šolomek, T.; Matile, S.; Vauthey, E. Long-Lived Triplet Charge-Separated State in Naphthalenediimide Based Donor–Acceptor Systems. *Chem. Sci.* **2021**, *12* (13), 4908–4915. https://doi.org/10.1039/D1SC00285F.

(23) Abet, V.; Szczypiński, F. T.; Little, M. A.; Santolini, V.; Jones, C. D.; Evans, R.; Wilson, C.; Wu, X.; Thorne, M. F.; Bennison, M. J.; Cui, P.; Cooper, A. I.; Jelfs, K. E.; Slater, A. G. Inducing Social Self-Sorting in Organic Cages To Tune The Shape of The Internal Cavity. *Angew. Chem. Int. Ed.* **2020**, *59* (38), 16755–16763. https://doi.org/10.1002/anie.202007571.

(24) Zhu, Q.; Qu, H.; Avci, G.; Hafizi, R.; Zhao, C.; Day, G. M.; Jelfs, K. E.; Little, M. A.; Cooper, A. I. Computationally Guided Synthesis of a Hierarchical [4[2+3]+6] Porous Organic 'Cage of Cages.' *Nat. Synth.* **2024**, 1–10. https://doi.org/10.1038/s44160-024-00531-7.

(25) Bera, S.; Dey, K.; Pal, T. K.; Halder, A.; Tothadi, S.; Karak, S.; Addicoat, M.; Banerjee, R. Porosity Switching in Polymorphic Porous Organic Cages with Exceptional Chemical Stability. *Angew. Chem. Int. Ed.* **2019**, *58* (13), 4243–4247. https://doi.org/10.1002/anie.201813773.

(26) Smith, P. A. S.; Dang, C. V. Prototropic Equilibrium of Imines. N-Benzylidene Benzylamines. *J. Org. Chem.* **1976**, *41* (11), 2013–2015. https://doi.org/10.1021/jo00873a027.

(27) Ciaccia, M.; Cacciapaglia, R.; Mencarelli, P.; Mandolini, L.; Stefano, S. D. Fast Transimination in Organic Solvents in the Absence of Proton and Metal Catalysts. A Key to Imine Metathesis Catalyzed by Primary Amines under Mild Conditions. *Chem. Sci.* **2013**, *4* (5), 2253–2261. https://doi.org/10.1039/C3SC50277E.

(28) Ciaccia, M.; Stefano, S. D. Mechanisms of Imine Exchange Reactions in Organic Solvents. *Org. Biomol. Chem.* **2014**, *13* (3), 646–654. https://doi.org/10.1039/C4OB02110J.

(29) Štacko, P.; Šolomek, T.; Klán, P. Electronic-State Switching Strategy in the Photochemical Synthesis of Indanones from o-Methyl Phenacyl Epoxides. *Org. Lett.* **2011**, *13* (24), 6556–6559. https://doi.org/10.1021/ol202892r.

(30) Peterson, P. W.; Shevchenko, N.; Alabugin, I. V. "Stereoelectronic Umpolung": Converting a p-Donor into a σ-Acceptor via Electron Injection and a Conformational Change. *Org. Lett.* **2013**, *15* (9), 2238–2241. https://doi.org/10.1021/ol400813d.